Food Chemistry: X 24 (2024) 101989

Contents lists available at ScienceDirect

Food Chemistry: X

journal homepage: www.sciencedirect.com/journal/food-chemistry-x

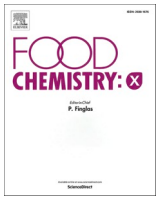

Comparative investigation of metabolite signatures and hypoadiposity effect between Dali tea and Yunkang tea

Mengwan Li [a,b,1], Dan Liu [a,b,1], Tingting Han [a,b], Juan Li [c], Linbo Chen [d], Daxiang Li [a,b,*], Zhongwen Xie [a,b,*]

[a] State Key Laboratory of Tea Plant Biology and Utilization, School of Tea and Food Sciences and Technology, Anhui Agricultural University, Hefei, Anhui 230036, PR China
[b] Joint Research Center for Food Nutrition and Health of IHM, Anhui Agricultural University, Hefei, Anhui 230036, PR China
[c] Center for Biotechnology, Anhui Agricultural University, Hefei, Anhui, 230036, PR China
[d] Tea Research Institute, Yunnan Academy of Agricultural Sciences, Menghai, Yunnan 666201, PR China

ARTICLE INFO

Keywords:
Camellia taliensis
Metabolomics
Characteristic compounds
Hypoadiposity

ABSTRACT

Dali tea (DLT) made by wild tea plant (*Camellia taliensis)* has been very popular in the market。However, the signature compounds and health benefits of DLT were not reported yet. To comprehensively understand metabolite signatures and potential health-function, the distinct metabolite signatures and hypoadiposity effect between DLT and Yunkang tea (YKT, made by *Camellia sinensis var assamica cv.* Yunkang 10) were comparative investigated. Our data found that catechins, and dimeric catechins were lower in DLT than YKT. In contrast, the levels of phenolic acid and amino acids were higher in DLT than YKT. An un-targeted metabolomics and a chemometric analysis indicated that flavonoid biosynthesis is a major pathway that distinguishes DLT from YKT. Additionally, chlorogenic acid, ellagic acid, arginine, tyrosine, and theanine were identified as characteristic metabolites of DLT. Furthermore, animal experiment showed that YKT performs better efficiency than DLT on alleviating hyperadiposity and renal damages in high-fat-diet induced obese mice.

1. Introduction

Tea is one of the most popular beverages consumed worldwide, and has shown multiple health benefits, including anti-obesity, hypoglycemic, and hypotensive (Li et al., 2019; Teng et al., 2018; Wu et al., 2022). Currently, commercial teas are mostly produced from the buds and leaves of two *Camellia* plants, named *Camellia sinensis* var. *sinensis* (Chinese variety) and *Camellia sinensis* var. *assamica* (Assam variety) (Liu et al., 2020; Meng et al., 2019). Historically, most of species in section *Thea* of *Camellia* have been used to make tea over the centuries. The natives of the regions where they grow have also consumed them for a long history. Tea plants originated in different regions and cultivated in different environments produce different metabolites and potential health benefits. One of the most important wild relatives of cultivated tea plants is *Camellia taliensis* (*C. taliensis*), which is an evergreen tree distributed in eastern and southwestern Yunnan province in China, and northern Myanmar. Researchers have reported that *C. taliensis* exhibits a wide range of abiotic stress resistance and biological resistance properties as their ideal alleles for tea plant breeding (Liu et al., 2012; Zhao et al., 2014). Zhang et al. has observed that *C. taliensis* has several genes might be related to stress response (Zhang et al., 2015). It was reported that *C. taliensis* is very closely related to Assam variety, a widely cultivated tea plant (Gao et al., 2008; Tien, 1992). Yunkang 10, a representative variety of Assam variety, has been used as a model tea plant for studying the transcription of *C. taliensis* (Zhang et al., 2015). It remains unclear, however, which characteristic metabolites and metabolic pathways between *C. taliensis* and Assam variety. In southwestern of China, *C. taliensis* has been cultivated for long time. Recently, tea made from *C. taliensis* (DLT) has been very popular and expensive on the market. Because of limited amount of product, the value of DLT is more than 10 times higher than tea made from cultivated tea plants (Liu et al., 2012). However, there is no data available to show that DLT has superior health benefits to the Assam tea plant made tea, such as YKT.

To reveal special chemical compositions and potential health-

* Corresponding authors at: State Key Laboratory of Tea Plant Biology and Utilization, School of Tea and Food Sciences and Technology, Anhui Agricultural University, Hefei, Anhui 230036, PR China.
E-mail addresses: dxli@ahau.edu.cn (D. Li), zhongwenxie@ahau.edu.cn (Z. Xie).
[1] These authors contributed equally.

https://doi.org/10.1016/j.fochx.2024.101989
Received 23 July 2024; Received in revised form 6 November 2024; Accepted 7 November 2024
Available online 9 November 2024

promoting properties of DLT, it is critical to comparatively identify the distinct metabolites and to evaluate health benefits between DLT and YKT. In our previous study, YKT exhibited a significant amelioration of the obesity complication in HFD-induced obese mice (Zhang, Gu, et al., 2020). In this study, we compared the chemical profiles, identified differential metabolites between DLT and YKT by using untargeted metabolomics strategy combined with chemometrics analysis, and evaluated their beneficial effects using a mouse model of obesity induced by HFD. This study will provide in-depth information of the metabolite profile and characteristic metabolites of DLT, and evaluate its potential health benefits comparing to YKT. These findings will serve as the basis for understanding characteristic chemical compounds and potential health benefits of DLT, and for reasonable utilization of Dali wild tea resources.

2. Material and methods

2.1. Chemicals

Chemical standards of chlorogenic acid and ellagic acid were purchased from Chem Faces (Wuhan, China). Chromatographic grade format and ACS grade of 5-sulfosalicylic acid dihydrate were purchased from Aladdin (Shanghai, China); chromatographic grade of acetonitrile and methanol were purchased from Sigma-Aldrich (St. Louis, MO, USA). The water used for UHPLC-Orbitrap-MS/MS was purchased from Watsons (Guangzhou, China).

2.2. Tea sample preparation for UHPLC-Orbitrap-MS/MS analysis

Tea plants of *Camellia taliensis* and Yunkang 10 (*Camellia sinensis* var. *assamica cv.*Yunkang 10), were cultivated in the National Germplasm Resources Center for Assam Tea Plant in Menghai County, Yunnan Province, China. One bud and two leaves were collected from the tea plants and were used to make green tea by a standard steamed protocol.

Tea extraction was prepared using a methanol and water solution at 70:30 ratio (*v*/v) followed a MS/MS analysis based on our previous method (Li et al., 2021; Li et al., 2022). Briefly, all samples were filtered through a 0.22 mm nylon filter, then were a diluted to 100 ng/mL of final concentration. The samples were tested together with an internal standard of 200 ng/mL. The quality control (QC) samples were obtained by mixing equal volumes of each sample analyzed in the current study in order to monitor the stability of the system in un-targeted metabolomics.

2.3. Quantification of chlorogenic acid and ellagic acid by UPLC

A method for quantification of chlorogenic acid and ellagic acid was developed following our previous method with a minor modification (Li et al., 2022). In short, approximate 200 mg of each tea powder was extracted by 9 mL of formic acid/methanol solution (5:95, *v*/v) for 65 min in a 50 °C water bath. After that, the samples were filtered through 0.22 μm nylon filters before injection into UPLC system. A volume of 2 μL of the sample solution was injected into quadruplicate. ACQUITY UPLC HSS T3 column with 1.8 m, 2.1 × 150 mm diameter was used to separate phenolic compounds, while the column temperature was maintained at 30 °C. A flow rate of 0.3 mL/min was maintained for mobile phase A (0.1 % formic acid, acetonitrile/water, 5: 95, v/v) and mobile phase B (0.1 % formic acid, water/acetonitrile, 5: 95, v/v). There were two wavelengths of 280 nm and 326 nm for ultraviolet detection. Every phenolic compound was subjected to seven calibration curves ranging from 3.125 μg/mL to 200 μg/mL in order to validate the stability of the method.

2.4. Quantification of arginine, tyrosine and theanine

Tea powder (100 mg) was mixed with 4 mL sulfosalicylic acid, and was under ultrasound solicitation for 40 min. After centrifugation at 12,000 rpm for 30 min, the supernatants were filtered through 0.22 m hydrophilic filters. Quantification of amino acids was conducted using a Hitachi L-8900 Amino Analyzer.

2.5. Animal experimental design and treatment

Male C57BL/6 J mice of 5 weeks of age, free of specific pathogens, were purchased from Gem Pharmatech Co., Ltd. (Nanjing, China), and were housed in cages at the laboratory animal facility center of Anhui Agricultural University. All cages were maintained at a constant temperature (23 °C ± 2 °C) and humidity (50 % ± 5 %) following a 12:12 h light-dark cycle from 8:30 a.m. to 8:30 p.m. Food and water were provided to all animals ad libitum. The mice were randomly assigned to 7 groups ($n = 12$) after adaptation for one week, including low fat diet feeding group (LFD), high fat diet feeding group (HFD), HFD supplement with 5 % DLT group (DLTL), HFD supplement with 7.5 % DLT group (DLTH), HFD supplement with 5 % YKT group (YKTL), HFD supplement with 7.5 % YKT group (YKTH), HFD supplement with 5 % DLT and 5 % YKT group (DLYK). Compared to the LFD (3.6 kcal/g), the HFD (5.1 kcal) contains 60 % of its energy from fat. Animal procedures were approved by the Institutional Animal Care and Use Committee of Anhui Agricultural University (ethical approval code: AHAU2022013).

In order to determine when DLT and YKT have a preventive effect on obesity complications, the body weight and body composition of mice was monitored weekly by using a scale and minispec LF90 (Bruker, Germany), respectively. At the end of the 12-week tea intervention, the mice were fasted for 12 h, and were then sacrificed under an overdose of chloral hydrate anesthesia (400 mg/kg, i.p). The peripheral blood was collected under anesthesia from the ophthalmic vein. Serum was obtained by centrifugation at 3000 rpm/min for 5 min at 4 °C then stored at −80 °C until use. The triglyceride (TG), total cholesterol (TC), and low-density lipoprotein cholesterol (LDL-C) levels in plasma were determined following the instructions of micro-testing kits (Nanjing Jiancheng Bioengineering Institute, Nanjing, China). A small part of liver and kidney tissues at the same position across groups of mice was rapidly collected and fixed in 10 % buffered formalin for histological analysis.

2.6. Un-targrt metabolomics analysis

A multivariate statistical analysis of the raw UHPLC-Orbitrap-MS/MS data was conducted using XCMS Online (http://xcmsonline.scripps.edu/) and the result was exported into Excel tables. A principal component analysis (PCA) and a partial least squares discrimination analysis (PLS-DA) were conducted using SIMCA-P 13.0. Approximately 200 permutations were performed to verify whether the PLS-DA model was overfitted. Using the PLS-DA model, VIP was calculated, along with fold change and *p*-value. For the determination of differential metabolites between DLT and YKT, the screening conditions were relative standard deviation (RSD) of 0.3, VIP greater than 1, *p*-value less than 0.05 and fold change (FC, FC=DLT/YKT) greater than or less than 1.5 (FC > 1.5 or FC < 1.5) (Zeng et al., 2019). By comparing RT, *m/z* with published literatures, HMDB (http://www.hmdb.ca/) (Wishart et al., 2022), PubChem (http://www.ncbi.nlm.nih.gov/pccompound/) (Kim et al., 2023), METLIN (http://metlin.scripps.edu/) (Liu et al., 2020) and Tea Metabolism Database (TMDB, http://pcsb.ahau.edu.cn:8080/TMDB/teaAction_search.action) (Yue et al., 2014), we preliminarily identified the potential differential metabolites. And then MetaboAnalyst 5.0 (https://www.metaboanalyst.ca/ (Pang et al., 2022) combined with KEGG pathway database (http://www.genome.jp/kegg/pathway.html) were used to generate heatmap and possible metabolic pathway map.

2.7. Histological analysis of liver and kidney tissues

Hematoxylin-eosin (HE) staining was conducted following previous

published protocol (Teng et al., 2018). Briefly, the liver and kidney tissues in paraffin were cut into 5 μm sections. The sections were stained with HE staining kit (Boster Biotech, Wuhan, China). The pictures were captured using a microscope (LEICA DM500, Wetzlar, Germany) and a camera (LEICA ICC50 W). The area of the hepatic lipid and glomeruli area were determined using Image-J2 software (NIH, Bethesda, MD, USA).

2.8. RNA isolation and real-time PCR analysis

To measure the expression of hepatic lipogenic gene in the liver samples, the total RNA was extracted using RNA-Easy isolation reagent (Vazyme, Nanjing, China). The cDNA was synthesized using HiScript II cDNA synthesis kit (Vazyme). Real-Time PCR analysis was performed according to our previous method (Xie et al., 2015) using AceQ qPCR SYBR Green kit (Vazyme). The primer sequences were listed in Table S1 in the supplemental material.

2.9. Statistical analysis

GraphPad Prism 8.0 was used to analyze other quantitative data, with a significance level set at $p < 0.05$. Data were mean ± SEM. There were multiple groups compared using one-way or two-way ANOVA with Tukey's test when necessary. The *t*-test was used to determine whether there was a significant difference between the two groups.

3. Results

3.1. Significant differences of metabolite profiles between Dali tea and Yunkang tea

A UHPLC-Orbitrap-MS/MS system was used to detect metabolites between Dali tea (DLT) and Yunkang tea (YKT). Based on the analysis of the typical total ion current chromatograms of tea samples (Fig. S1), 3127 and 4512 ion features were generated by positive and negative ion model, respectively. The typical chromatograms and mass spectrograms for DLT and YKT samples are illustrated in Fig. S2. An unsupervised PCA analysis was initially conducted to examine intra- and inter-class differences between DLT and YKT. The results revealed that the samples from DLT and YKT were separated each other, and were clustered into an individual group, respectively. In addition, the quality control (QC) samples were gathered together, indicating the stability and reliability of our metabolomics analysis. Moreover, the DLT and YKT samples were clearly distinguished, indicating significant differences in chemical profiles between DLT and YKT both in positive and negative ion modes (Fig. 1A, D). To determine the metabolites with the greatest differences, the supervised PLS-DA model was applied. The results showed that the DLT samples were clustered in the quadrant I and IV, and the YKT samples were grouped in the quadrant II and III (Fig. 1B, C). The result indicated again that DLT and YKT exhibit distinct chemical profiles. In addition, R^2X, R^2Y and Q^2 were calculated as 0.545, 0.987 and 0.931 in positive model and 0.973, 0.999, 0.969 in negative model, respectively, indicating that the models were established successfully without overfitting. The permutation test also showed that there was no overfitting in positive and negative models, respectively (Fig. 1C, F).

3.2. Characteristic metabolites between DLT and YKT

A criterion with VIP value more than 1 (VIP > 1), *p* value in nonparametric test less than 0.05 ($P < 0.05$) and fold change more than or less than 1.5 (FC > 1.5 or FC < 1.5) was selected as screen potential differential metabolites. Based on the comparison of RT, *m/z* values, secondary mass spectrometry fragments, various metabolome databases and published literature, a total of sixty-one differentiated metabolites between DLT and YKT were identified, which including seven catechins, seven dimeric catechins, twenty flavonols and flavone glycosides, two hydrolyzable tannins, seven phenolic acids, four amino acids, two organic acids, five alkaloids, and seven other compounds (Table 1). Based on abundant of 61 differential metabolites, a heat map was generated to provide an overview of the abundance of differentiated metabolites between DLT and YKT (Fig. 2).

3.2.1. Catechins

The catechins are main polyphenol in the teas, exhibit the strong

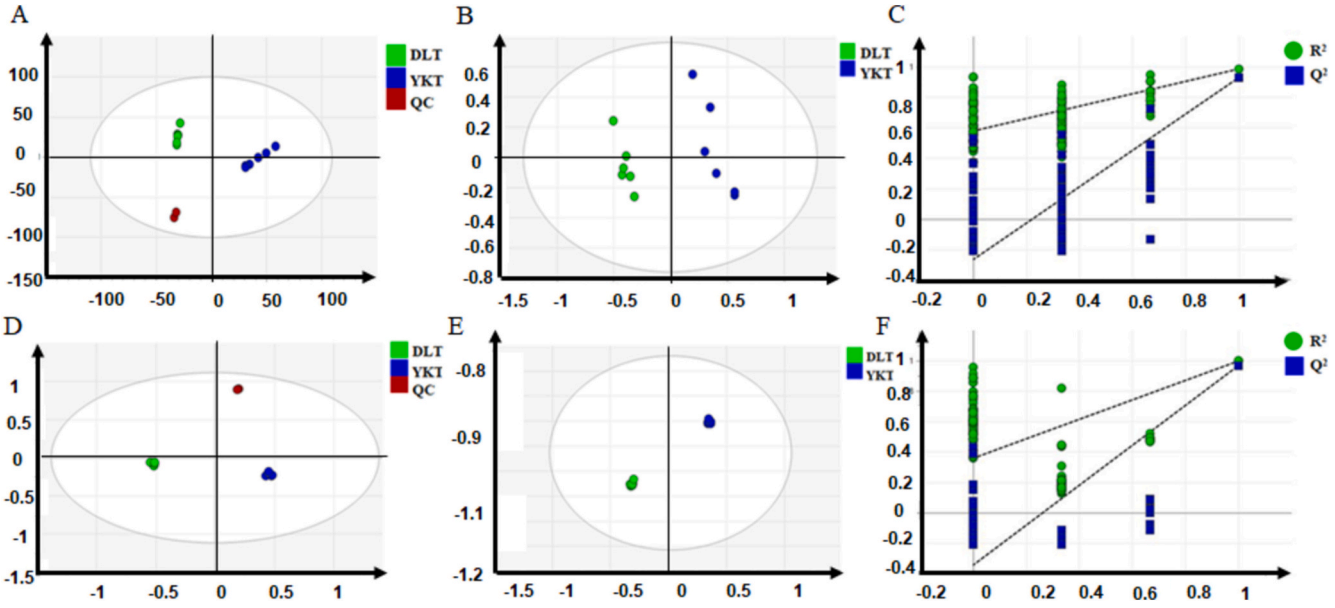

Fig. 1. Multivariate statistical analysis between DLT (Dali green tea) and YKT (Yunkang green tea). A and D: PCA score plot of positive ($R^2X = 0.836$, $Q^2 = 0.737$) and negative ($R^2X = 0.887$, $Q^2 = 0.863$) ionization mode, respectively; B and E: PLS-DA score plot of positive ($R^2X = 0.545$, $R^2Y = 0.987$, $Q^2 = 0.931$) and negative ($R^2X = 0.973$, $R^2Y = 0.999$, $Q^2 = 0.969$) ionization mode, respectively; C and F: cross-validation plot of PLS-DA model of positive (intercepts of R^2 and Q^2 were 0.579 and − 0.268, respectively) and negative (intercepts of R^2 and Q^2 were 0.358 and − 0.347, respectively) ionization mode, respectively. Data are presented as the mean ± SEM ($n = 6$). (For interpretation of the references to colour in this figure legend, the reader is referred to the web version of this article.)

Table 1
The differentiated metabolites between DLT and YKT.

Compound name	RT [min]	Measured mass	Theoretical mass	Formula	Adduct	Fragment ion
Catechins						
(−)-Epiafzelechin 3-gallate	4.08	426.09484	426.0945335	$C_{22}H_{18}O_9$	[M + H]+	139,123,287,163
Epigallocatechin gallate	4.247	458.0834	458.0843627	$C_{22}H_{18}O_{11}$	[M + H]+	139,153,163
(−)-Epigallocatechin 3-(4-methyl-gallate)	3.922	472.09895	472.1011096	$C_{23}H_{20}O_{11}$		
Catechin	3.659	290.0781	290.0795864	$C_{15}H_{14}O_6$	[M-H]-	125,137,109,161
Epicatechin	3.775	290.0781	290.0795864	$C_{15}H_{14}O_6$		
Epicatechin 3-(3-methylgallate)	4.087	456.10424	456.106195	$C_{23}H_{20}O_{10}$		
(−)-Epiafzelechin	4.104	274.08305	274.0846718	$C_{15}H_{14}O_5$		
Dimeric catechins						
Theasinensin C	4.427	610.13002	610.1328036	$C_{30}H_{26}O_{14}$	[M-H]-	271,300,255
Epicatechin-(4β- > 8)-gallocatechin	3.838	594.13678	594.1367922	$C_{30}H_{26}O_{13}$	[M + H]+	127,139,151,163
Epigallocatechin-(4β- > 8)-epicatechin 3-*O*-gallate	3.912	746.14757	746.1488475	$C_{37}H_{30}O_{17}$		
Epigallocatechin-(4β- > 8)-epigallocatechin-3-*O*-gallate	3.604	762.1402	762.1437621	$C_{37}H_{30}O_{18}$	[M-H]-	125,177,137
Procyanidin B1	3.903	578.14039	578.1429744	$C_{30}H_{26}O_{12}$	[M-H]-	125,137,109,161
Epiafzelechin 3-*O*-gallate-(4β- > 6)-epigallocatechin 3-*O*-gallate	4.127	882.16058	882.1648914	$C_{44}H_{34}O_{20}$		
Epiafzelechin-(4β- > 8)-epicatechin 3,3′-digallate	4.131	866.16569	866.1699768	$C_{44}H_{34}O_9$		
Flavonoids and flavonoid glycosides						
Isovitexin 2″-glucoside	3.914	594.15766	594.1579215	$C_{27}H_{30}O_{15}$		
Kaempferol 3-(2″,6″-di-(e)-p-coumarylglucoside)	4.815	740.17328	740.1735716	$C_{39}H_{32}O_{15}$		
Myricetin	3.806	318.03722	318.0370187	$C_{15}H_{10}O_8$	[M + H]+	319,153,217,245
Quercetin 3-galactoside	3.429	464.09518	464.0949274	$C_{21}H_{20}O_{12}$	[M + H]+	319,153,217,245
(−)-Epigallocatechin 3-cinnamate	4.354	436.11457	436.1163658	$C_{24}H_{20}O_8$		
Assamicain C	3.798	916.1663	916.1703707	$C_{44}H_{36}O_{22}$		
Kaempferol 3-[4″-(*p*-coumaroylglucosyl)rhamnoside]	4.17	740.19313	740.1957977	$C_{36}H_{36}O_{17}$		
Luteolin 7-methyl ether	4.821	300.06241	300.0639364	$C_{16}H_{12}O_6$		
Naringenin	4.788	272.06763	272.0690218	$C_{15}H_{12}O_5$	[M-H]-	116,203,74,62,142,130,225
Pollenitin	4.125	316.05736	316.058851	$C_{16}H_{12}O_7$		
Theaflavate B	4.231	700.14051	700.1433682	$C_{36}H_{28}O_{15}$		
trans-3,3′,4′,5,5′,7-Hexahydroxyflavanone	3.598	320.05187	320.0537656	$C_{15}H_{12}O_8$	[M-H]-	125,193,57,137,175,151,191
Rutin	3.841	610.15269	610.1528361	$C_{27}H_{30}O_{16}$	[M + H]+	303,85,71
Vicenin 2	3.616	594.15796	594.1579215	$C_{27}H_{30}O_{15}$		
Hyperin 6″-[glucosyl-(1- > 3)-rhamnoside]	3.82	772.20296	772.2067562	$C_{33}H_{40}O_{21}$		
Kaempferol 3-(6″-rhamnosylsophoroside)	3.869	756.20816	756.2118416	$C_{33}H_{40}O_{20}$	[M-H]-	285,255,227
Kaempferol 3-[glucosyl-(1- > 3)-rhamnosyl-(1- > 6)-galactoside]	3.731	756.20826	756.2118416	$C_{33}H_{40}O_{20}$		
Quercetin 3-(3r-glucosylrutinoside)	3.753	772.20328	772.2067562	$C_{33}H_{40}O_{21}$		
Quercetin 3-α-l-rhamnopyranoside	3.55	448.10017	448.1000128	$C_{21}H_{20}O_{11}$		
Quercetin	4.013	302.04235	302.0421041	$C_{15}H_{10}O_7$	[M + H]+	303,257,275,285
Hydrolyzable tannins						
1,2-di-galloyl-β-D-glucopyranose	1.742	484.08177	484.0858534	$C_{20}H_{20}O_{14}$	[M-H]-	125,169,211,62
1-galloyl-4,6-(s)-hexahydroxydiphenoyl-β-D-glucopyranose	3.633	634.07841	634.0811619	$C_{27}H_{22}O_{18}$	[M-H]-	137,125,327,83
Phenolic acids						
Chlorogenic acid	4.112	354.09086	354.0945335	$C_{16}H_{18}O_9$		
3-*p*-Coumaroylquinic acid	1.522	338.09762	338.0996189	$C_{16}H_{18}O_8$		
4-Hydroxybenzoic acid	4.46	138.03129	138.0322424	$C_7H_6O_3$	[M-H]-	93,137,108
Ellagic acid	3.633	302.00477	302.0068154	$C_{14}H_6O_8$	[M-H]-	62,281,117,131,129
Quinic acid	3.669	192.06264	192.0639364	$C_7H_{12}O_6$		
Shikimic acid	3.816	174.05213	174.0533717	$C_7H_{10}O_5$	[M-H]-	93,173,63,62
Succinic acid	1.359	118.02637	118.027157	$C_4H_6O_4$		
Amino acids						
L-Arginine	3.547	174.11173	174.1111272	$C_6H_{14}N_4O_2$		
L-Phenylalanine	1.962	165.0789	165.0784301	$C_9H_{11}NO_2$		
L-Theanine	1.576	174.09985	174.1009906	$C_7H_{14}N_2O_3$		
L-Tyrosine	1.253	181.07342	181.0744415	$C_9H_{11}NO_3$		
Organic acids						
Benzoic acid	3.642	122.0366	122.036231	$C_7H_6O_2$	[M + H]+	123,122,107
Isocitric acid	1.249	192.0264	192.0275508	$C_6H_8O_7$		
Alkaloids						
2-Acetylpyrazine	1.213	122.04726	122.0474644	$C_6H_6N_2O$		
Guanine	1.246	151.04949	151.0488613	$C_5H_5N_5O$		
Theacitrin C	3.849	912.13417	912.1390706	$C_{44}H_{32}O_{22}$		
Theogallin	1.476	344.07402	344.0737981	$C_{14}H_{16}O_{10}$	[M + H]+	153,125,143,79
1,2,3-Trihydroxybenzene	1.872	126.03128	126.0322424	$C_6H_6O_3$	[M-H]-	125,88,69,97
Other compounds						
Ascorbic acid	1.114	176.03127	176.0326362	$C_6H_8O_6$		
alpha-Linolenic acid	7.53	278.22327	278.2251285	$C_{18}H_{30}O_2$	[M-H]-	121,209,120,122
Linoleic acid	10.093	280.23929	280.2407786	$C_{18}H_{32}O_2$	[M-H]-	139,62,119,124,163,187
Oleic acid	10.986	282.25492	282.2564286	$C_{18}H_{34}O_2$		
Camelliagenin A	9.165	474.36925	474.3714583	$C_{30}H_{50}O_4$		
Theasapogenol E	9.132	504.34349	504.3456374	$C_{30}H_{48}O_6$		
cis-3-Hexenyl formate	4.532	128.08321	128.084278	$C_7H_{12}O_2$		

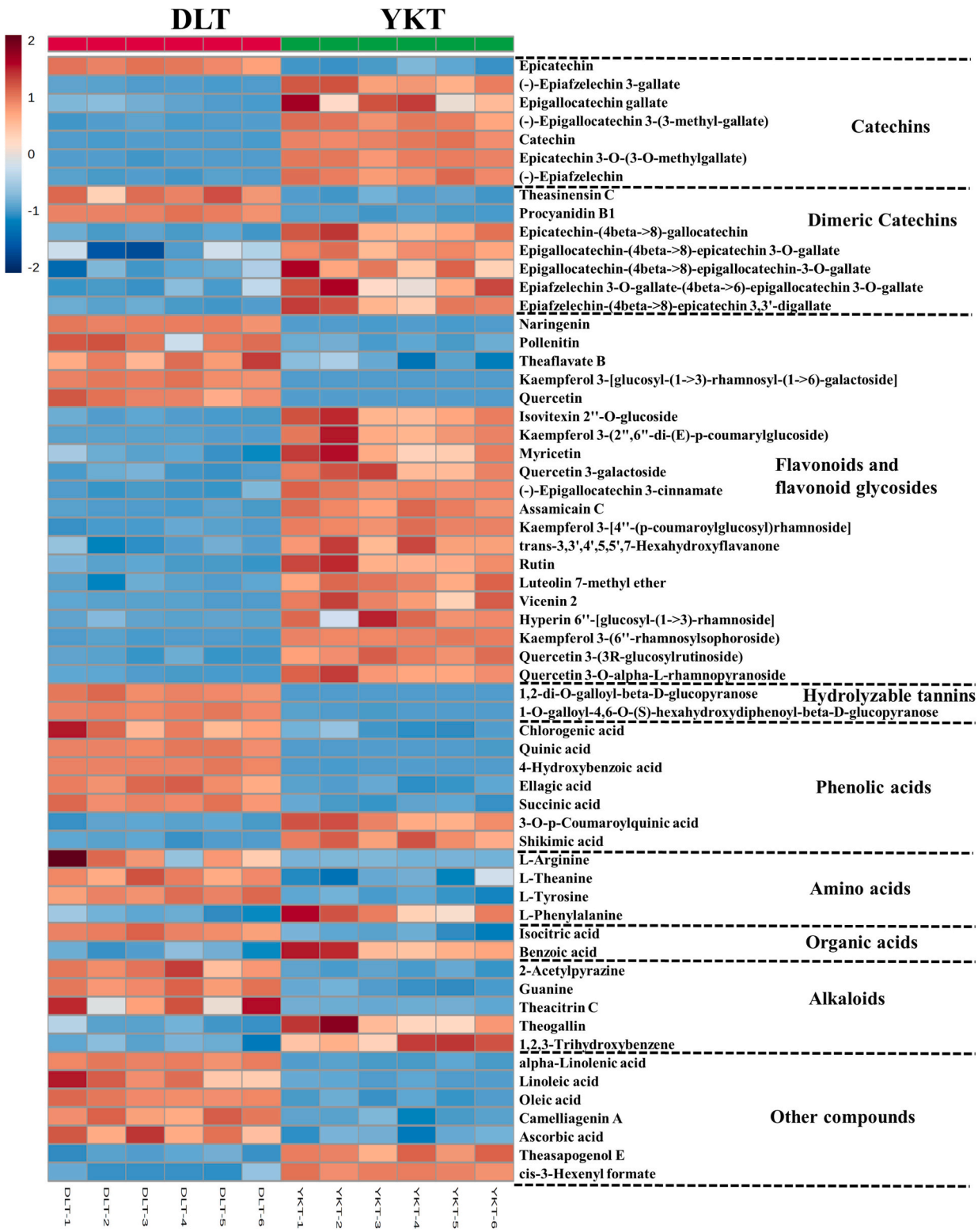

Fig. 2. Heat-map of the metabolite contents between YKT and DLT.

antioxidant properties and contribute to bitter flavor. In this study, the following catechins were putatively identified and were listed as (−)-epiafzelechin3-gallate, epigallocatechin gallate, (−)-epigallocatechin 3-(4-methyl-gallate), catechin, epicatechin, epicatechin 3-(3-methylgallate), and (−)-epiafzelechin. Specifically, epicatechin levels in DLT were higher than those in YKT as shown in the heat map. However, the levels of other catechins, including (−)-epiafzelechin 3-gallate, epigallocatechin gallate, (−)-epigallocatechin 3-(4-methyl-gallate), catechin, epicatechin 3-(3-methylgallate), and (−)-epiafzelechin, were lower in DLT than that in YKT.

3.2.2. *Dimeric catechins*

Seven characteristic dimeric catechins were identified between DLT and YKT, which as shown in Table 1. There are only two dimeric

catechins in DLT that exhibit greater abundance than those in YKT, namely theasinensin C and procyanidin B1. While epicatechin-(4β- > 8)-gallocatechin, epigallocatechin-(4β- > 8)-epicatechin 3-gallate, epigallocatechin-(4β- > 8)-epigallocatechin-3-gallate, epiafzelechin 3-gallate-(4β- > 6)-epigallocatechin 3-gallate, and epiafzelechin 3,3′-digallate displayed lower level in DLT than in YKT.

3.2.3. Flavonol and flavone glycosides

There is a large family of compounds with bioactive properties known as flavonols and flavone glycosides. The metabolomics analysis data revealed that there were four flavonols and flavone glycosides that were more abundant In DLT than in YKT. A putative identification of these compounds was made as naringenin, pollenitin, theaflavate B, and kaempferol 3-[glucosyl-(1- > 3)-rhamnosyl-(1- > 6)-galactoside]. While isovitexin 2"-O-glucoside, kaempferol 3-(2″,6″-di-(e)-p-coumarylglucoside), myricetin, quercetin 3-galactoside, (−)-epigallocatechin 3-cinnamate, assamicain C, kaempferol 3-[4″-(p-coumaroylglucosyl) rhamnoside], luteolin 7-methyl ether, trans-3,3′,4′,5,5′,7-hexahydroxyflavanone, rutin, vicenin 2, hyperin 6″-[glucosyl-(1- > 3)-rhamnoside], kaempferol 3-(6″-rhamnosylsophoroside), quercetin 3-(3r-glucosylrutinoside), quercetin 3-α-l-rhamnopyranoside, and quercetin are lower in DLT when compared to YKT.

3.2.4. Hydrolyzable tannins

The metabolic data demonstrated that there are two hydrolysable tannins in DLT, and their relative abundance is significantly higher than that in YKT. These two tannins were putatively identified as 1,2-di-galloyl-β-D-glucopyranose, and 1-galloyl-4,6-(*S*)-hexahydroxydiphenoyl-β-D-glucopyranose (Fig. 2). In terms of MS intensities, especially 1-galloyl-4,6-(s)-hexahydroxydiphenoyl-β-D-glucopyranose exhibited the 427-fold higher in DLT than in YKT.

3.2.5. Phenolic acids

DLT and YKT extracts contain various amounts of phenolic acids. In general, DLT possesses much higher levels of phenolic acids than YKT, which including chlorogenic acid, 4-hydroxybenzoic acid, ellagic acid, quinic acid, and succinic acid (Fig. 2). Additionally, DLT displayed lower levels of 3-*p*-coumaroylquinic acid and shikimic acid than YKT.

3.2.6. Amino acids and organic acids

The metabolic analysis results showed that DLT contained relatively higher levels of L-arginine, L-theanine, and L-tyrosine than that of YKT (Table 1). The level of *L*-phenylalanine, a single metabolite, was lower in DLT than in YKT (Fig. 2). Interestingly, the organic acids in DLT and YKT differ greatly. DLT (Table 1) has higher isocitric acid and lower benzoic acid levels than that of YKT (Fig. 2).

3.2.7. Alkaloids and other compounds

Theobromine and caffeine, two alkaloids found in tea plants, have been extensively studied. In this study, 2-acetylpyrazine, guanine, and theacitrin C levels were higher in DLT than in YKT (Table 1), whereas theogallin, and 1,2,3-trihydroxybenzene levels were lower in DLT than in YKT (Fig. 2). Among the other compounds, there were seven differential metabolites between DLT and YKT. The DLT contained higher levels of alpha-linolenic acid, linoleic acid, oleic acid, camelliagenin A, and ascorbic acid than the YKT. There was a lower content of theasapogenol E, and cis-3-hexenyl formate in DLT than in YKT (Fig. 2).

3.3. Quantification key metabolites in DLT

Un-target metabolomics analysis revealed that DLT exhibited significantly relative higher amount of chlorogenic acid, ellagic acid, arginine, L-tyrosine, and L-theanine than that of YKT. In order to further confirm those findings, absolutely quantitative analysis is essential. Therefore, UPLC and an amino acid Analyzer were used to quantify chlorogenic acid, ellagic acid, arginine, tyrosine, and L-theanine by running with those standard chemicals. Representative chromatograms of UPLC for the mixed standard solution containing chlorogenic acid and ellagic acid, DLT sample and YKT sample are showing as Fig. S3. The quantified data showed that DLT contains higher amount of chlorogenic acid, ellagic acid, arginine, tyrosine, and theanine than that of YKT (Fig. 3). These results are generally consistent with the chemical profile data.

3.4. Metabolic pathway analysis between DLT and YKT

The analysis of metabolic pathways based on differential metabolites helps us to understand how metabolic pathways are enriched between DLT and YKT. Fig. 4 illustrates an enrichment analysis of DLT and YKT metabolic pathways. Data for the enrichment metabolic pathways were plotted with log of the significance (*p*-value) as the ordinate, and with metabolic pathway impact as the abscissa. In this study, we observed that the differential metabolites between DLT and YKT were mainly enriched in flavonoid biosynthesis (Fig. 5). This is the most influential metabolic pathway, which has a pathway impact>0.18 and a − log (*p*-value) > 15.5. Based on analysis of flavonoid biosynthesis pathway, we found that chorismic acid is a key intermediate in the synthesis of *p*-coumaric acid and tyrosine. The precursor of coumaroyl-CoA is tyrosine, which promotes the production of flavonoids (Wei et al., 2012) In this pathway, the downstream metabolites are tyrosine and 3-*p*-coumaroylquinic acid, which were significantly higher in DLT. A series of enzymes, including chalcone synthase (CHS), chalcone isomerase (CHI), dihydroflavonol 4-reductase (DFR), anthocyanin synthetase (ANS) and UDP-glucosyl transferase (UGT), catalyze phenylalanine to produce dihydrokaempferol, as well as catechins, dimeric catechins, flavonols, and flavone glycosides (Pollastri & Tattini, 2011; Wang et al., 2017; Wei et al., 2012). Dihydrokaempferol is catalyzed by ANS to form colorless leucopelargonidin, which is the precursor of kaempferol. While the kaempferol is further glycosylated to form stable kaempferol glycosides, such as kaempferol 3-(2″,6″-di-(*E*)-p-coumarylglucoside, kaempferol 3-[4″-(p-coumaroylglucosyl) rhamnoside], kaempferol 3-(6″-rhamnosylsophoroside), kaempferol 3-[glucosyl-(1- > 3)-rhamnosyl-(1- > 6)-galactoside]. This glycosylated pathway is further supported by metabolic data, which showed that the kaempferol glycosides except kaempferol 3-[glucosyl-(1- > 3)-rhamnosyl-(1- > 6)-galactoside] were lower in DLT than YKT. Additionally, dihydroquercetin is a direct precursor of quercetin. Glycosylated quercetin leads to form stable quercetin glycosides, including quercetin 3-galactoside, quercetin 3-(3r-glucosylrutinoside), quercetin 3-α-l-rhamnopyranoside, and rutin, which all were lower in DLT than in YKT. In DLT, a number of metabolites involved in flavonoid biosynthesis were lower than in YKT, except for quercetin, epicatechin, kaempferol 3-(2″,6″-di-(e)-p-coumarylglucoside), procyanidin B1, and theasinensin C. Fig. 5 illustrates how the flavonoid biosynthesis pathway is suppressed in DLT to decreased production of kaempferol glycosides, quercetin glycosides, myricetin glycosides, apigenin glycosides, catechins. Decrease in quercetin-based flavonol glycosides would result in a decrease in dimeric catechins in DLT. There are fewer precursors available for the biosynthesis of flavonoid compounds in DLT due to the extensively suppressed flavonoid pathway. Therefore, polycondensation of dimeric catechin monomers may be further inhibited in DLT. Therefore, we found that high phenolic acid compounds are closely correlated to DLT. This study found that the metabolites of phenolic acids, such as chlorogenic acid, 3-*p*-coumaroylquinic acid, ellagic acid, quinic acid, and succinic acid, were more abundant in DLT compared to YKT (Fig. 5).

3.5. YLT shows better hypoadiposity effects than DLT in HFD induced obese mice

C57BL/6 J mice are widely used for high-fat diet (HFD) induced obesity. Our results showed that HFD feeding for 12 weeks led to a significant increase in body weight and fat mass ratio when compared

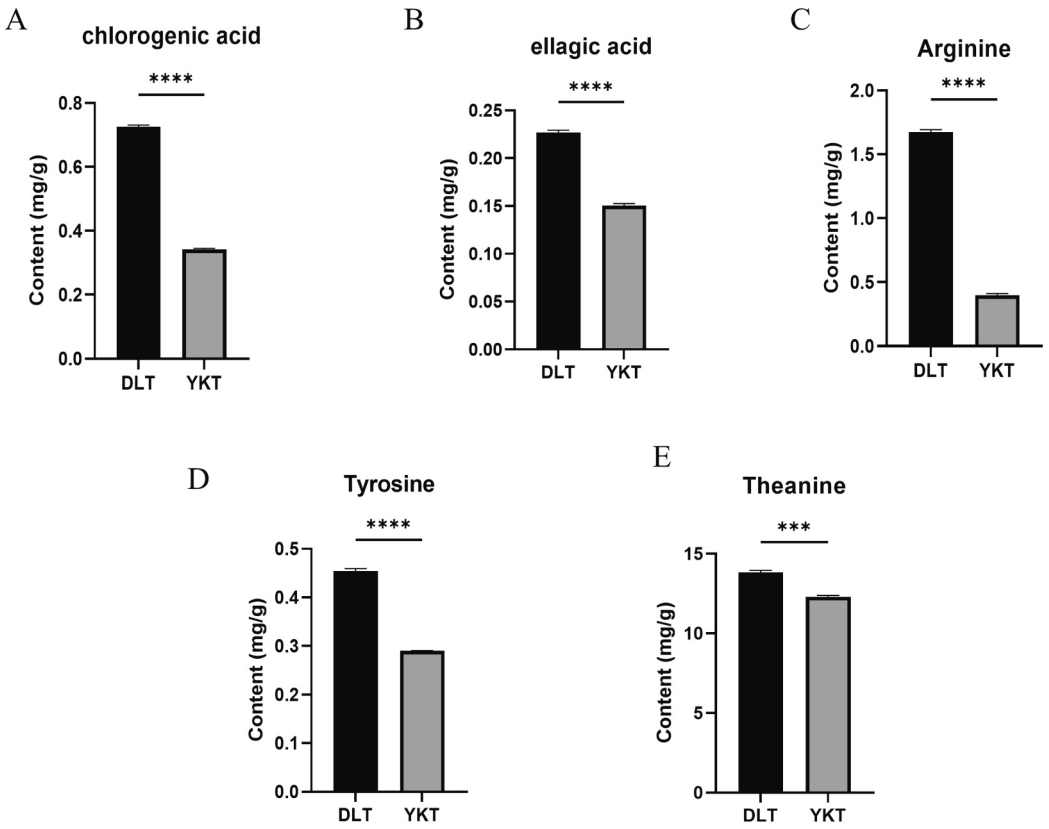

Fig. 3. Quantification of phenolic acids and amino acids between DLT and YKT.
*** $p < 0.001$, **** $p < 0.0001$ data are presented as the mean ± standard ($n = 3$).

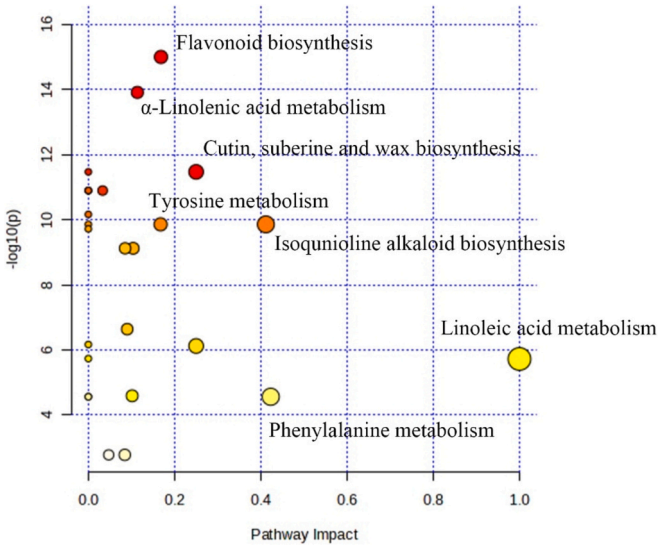

Fig. 4. Pathway analyses between DLT and YKT.
The y-axis (−log (*p*-value)) and x-axis represent the significance of the pathway and pathway impact between DLT and YKT, respectively.

with LFD feeding. However, dietary supplementation with DLT and YKT, significantly reduced the body weight and fat mass ratio in comparison with HFD mice (Fig. 6 A, B). Furthermore, a dose-dependent reduction in body weight and fat mass ratios was observed with DLT and YKT treatment. Interestingly, YKT proved to be more effective on suppressing of adiposity than DLT at the same dosage. In addition, dietary supplements of both DLT and YKT improved the lean mass ratio compared to HFD group of mice (Fig. 6C). HFD induced obese mice show markedly elevated plasma lipid levels, including LDL-C, TC, and TG (Fig. 6D-F). A higher dose of both DLT and YKT exerted a greater effect on decreasing those hyperlipidemia indexes than a lower dose. And again, YKT treated mice showed more effectively than DLT at the same dose.

Liver is a key organ for lipid metabolism. Next, the key genes for lipogenic regulation were measured using a Real-Time PCR approach. The results showed that DLT and YKT both inhibit *Ppar γ* expression in liver of HFD-mice. However, there is no difference in inhibitory effects (Fig. 7A). Furthermore, DLT and YKT intervention significantly decrease *C/ebp α*, *Srebp-1c* and *Fas* expression. Interestingly, YKT exhibits better inhibitory effects that DLT (Fig. 7B-D). In general, YLT exhibited more profound efficiency on alleviating hyperadiposity than DLT.

3.6. YKT and DLT prevent fatty liver and renal lesions in HFD induced obese mice

Obesity often accompanies fatty liver and kidney abnormality. Liver sectioning data showed that both YKT and DLT treatment significantly prevented lipid dispersition in hypercyte (Fig. 8 A-F). Quantification analysis indicated that there is no statistic deference between YKT and DLT (Fig. 8 G). HFD induced obese mice also has diabetic syndrome, and develops diabetic Nephropathy, consequently causes glomeruli lesions. In our study, renal HE staining displayed that HFD mice exhibited hyalinoid lesions of the mesangial matrix (Fig. 9b) and significantly increased glomerular area (Fig. 4G) when compared to the WT group. However, the intervention with both YLT and DLT mitigate abnormal renal hypertrophy and enhancing glomerular structural integrity (Fig. 9C-F). Again, YKT showed better preventive effects of renal lesions than that of DLT (Fig. 9G).

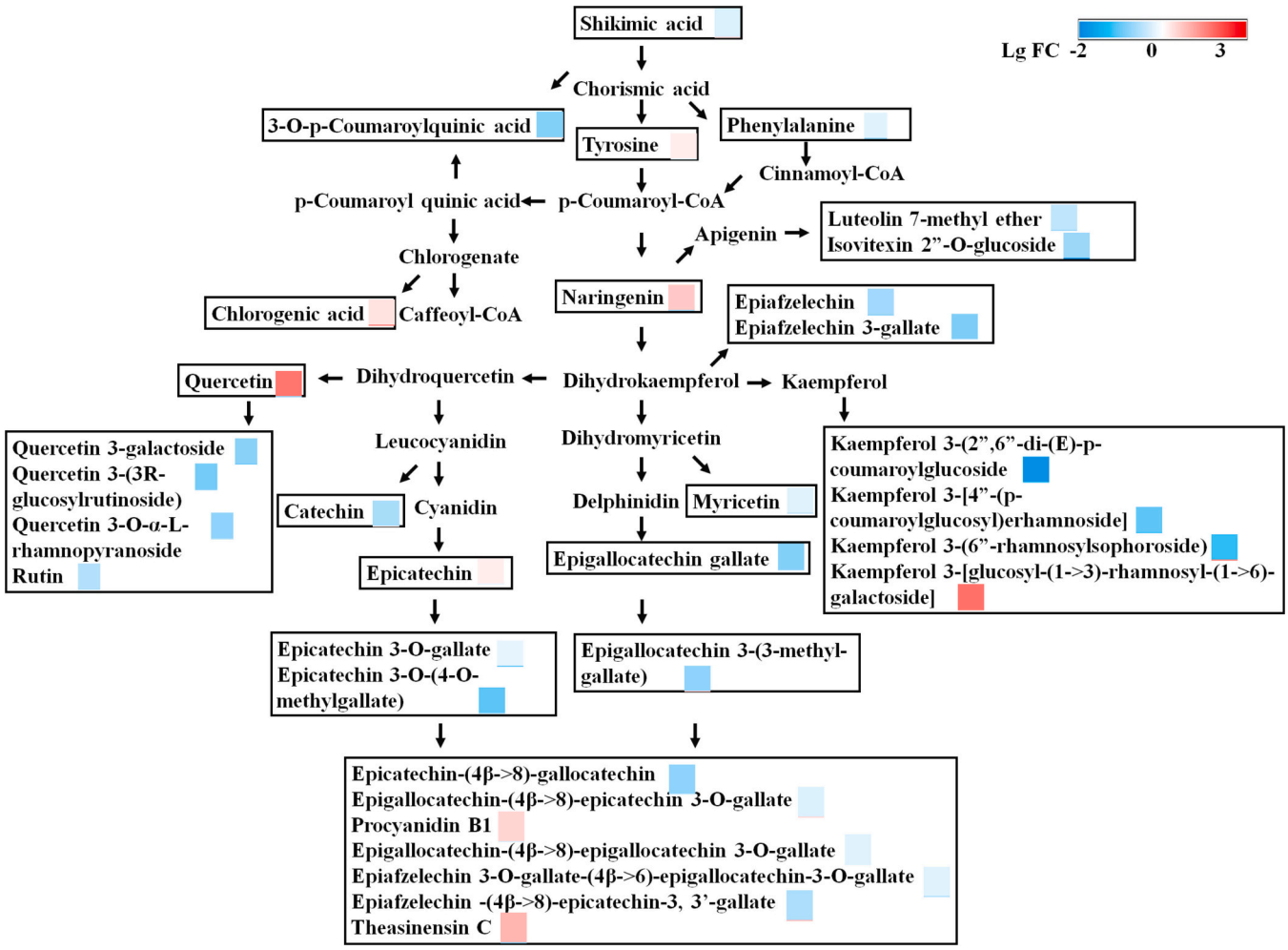

Fig. 5. Metabolic pathways of flavone and flavonol biosynthesis and amino acid biosynthesis in DLT and YKT.
Red or blue boxes represent values that were higher or lower than the mean value, respectively. (For interpretation of the references to colour in this figure legend, the reader is referred to the web version of this article.)

4. Discussion

Dali species (*Camellia taliensis*) is widely recognized as wild relative of cultivated tea plants. Published papers have reported that Dali species is a closely related wild species of Assam variety (*Camellia sinensis* var. *assamica*) (Gao et al., 2008; Zhang et al., 2015). In addition, Yunkang 10, a representative cultivar of Assam variety, has been used as a control model tea plant for studying the transcription and evolution of *C. taliensis* (Zhang et al., 2015; Zhao et al., 2014). Until now, because of the availability, DLT has been less investigated. Zhu et al. found a new flavan-3-ol dimer from green tea produced from *C. taliensis* (Zhu et al., 2012). Recently, Chen et al. reported a new hydrolyzable tannin with potent antioxidant and α-glucosidase inhibitory activity from black tea produced from *C. taliensis* (Xia et al., 2017). However, there is no report of metabolic profiles and potential hypoadiposity of DLT compared to YKT. This research provided a first set of data to identify characteristic compounds and to evaluate hypoadiposity effect of DLT compared to YKT. This set of data also presents a possible clue of chemical pathway evolution when *C. taliensis* in the process of domestication.

In this study, a total of sixty-one differentiated metabolites were putatively identified between DLT and YKT. Previously, Zhu et al. and Gao et al. reported that both DLT and YKT contain rich catechins, and DLT has less catechins than YKT (Gao et al., 2008; Zhu et al., 2012). YKT is also reported to have a higher percentage of epigallocatechin gallate (EGCG), the principal component of catechins, than DLT (Gao et al., 2008). Generally, our results are consistent with those reports. However, this study further found that DLT exhibits lower level of most of catechins and dimeric catechins identified than that of YKT. As one of the most popular health beverages, tea plants have ability to accumulate high amount of catechins, as well as to maintain their suitability during tea processing (Chen et al., 2023). One possible reason is that catechins synthesis pathway was enhanced in the domestication process from wild Dali species to cultivated Assam variety.

Arginine and tyrosine are hydrophilic amino acids. Our data showed that arginine and tyrosine are more abundant in DLT than in YKT. Previous researches reported that late embryogenesis abundant (*LEA*) gene is linked to hydrophilic amino acids. And LEA protein, a protein found in plants, has exceptional resistance to stress, particularly to cold (Garay-Arroyo et al., 2000; Swaminathan et al., 2019). The presence of *LEA* genes in *C. taliensis* is significantly higher than in *C. sinensis* var. *assamica*, which may explain the observed greater abiotic stress in wild *C. taliensis* (Zhang et al., 2015). High amount of arginine and tyrosine in DLT may contribute to resistance to abiotic stress of Dali tea. Moreover, we found that there were more phenolic acid metabolites in DLT than in YKT. Several studies have suggested that chlorogenic acid is a key metabolite biomarker that may be helpful in improving wolfberry tolerance to salt-alkaline stress, as well as honeysuckle (*Lonicera japonica*) tolerance (Liang et al., 2022; Yan et al., 2016). In cultivated lettuces and eggplants, human selection has reduced the level of phenolic acids such as chlorogenic acid and quinic acid, which impart a

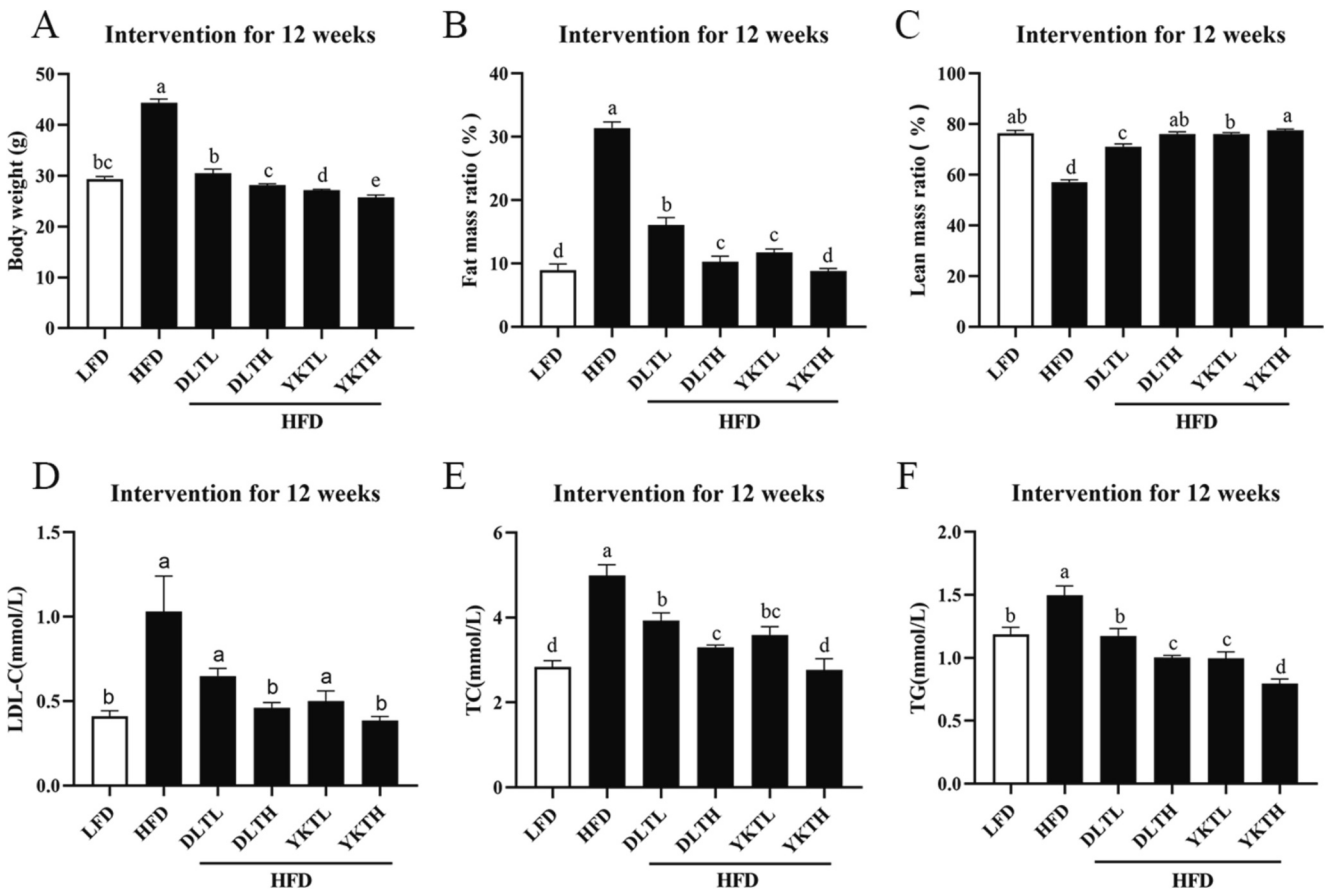

Fig. 6. Distinct hypoadiposity effects between DLT and YKT in HFD-fed mice.
Body weight (A), fat mass ratio (B), lean mass ratio (C), LDL-C (D), TC (E), TG (F). a, b, c, d Different lowercase letters in each column indicate significant differences among groups ($p < 0.05$). All data are presented as mean ± SEM ($n = 12$).

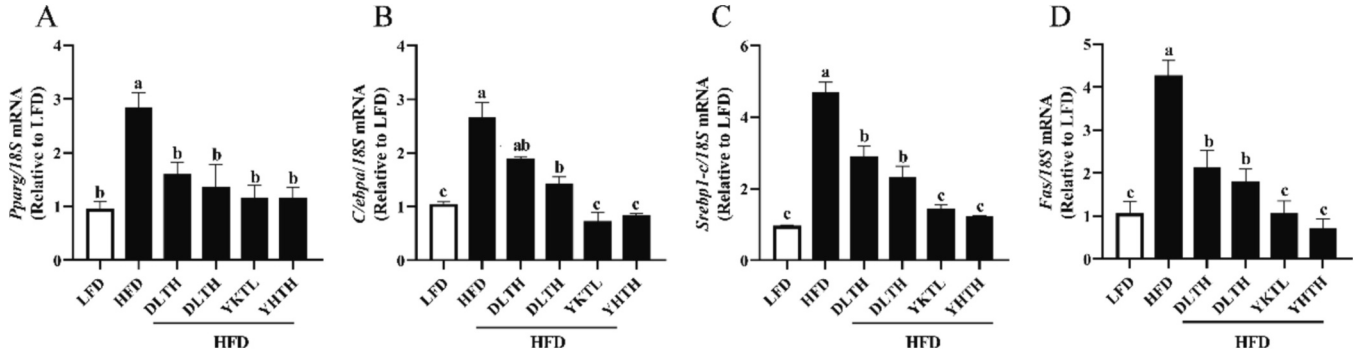

Fig. 7. Distinct inhibitary effects for lipogenic gene expression between DLT and YKT in HFD-fed mice.
The expression level of *Ppar γ* (A), *C/ebp α* (B), *Srebp-1c* (C) and *Fas* (D) in liver were assessed using qPCR. Different lowercase letters in each column indicate significant differences among groups ($p < 0.05$). Data are expressed as mean ± SEM ($n = 3$).

pungent flavor (Meyer et al., 2015; Zhang, Alseekh, et al., 2020). High number of phenolic acids in DLT also suggested a decease trend in the human selection process of Dali tea cultivation. Based on both untargeted and targeted metabolomic data, we identified chlorogenic acid, quinic acid, theanine, arginine, and tyrosine as the key characteristic metabolites of DLT.

DLT is noteworthy for its high concentration of hydrolyzed tannins, which contribute to its glycine taste (Gao et al., 2008; Zhu et al., 2012). Our data indicated that two hydrolyzable tannins including 1,2-di-galloyl-β–glucopyranose, and 1-galloyl-4,6-(s)-hexahydroxydiphenoyl-β-D-glucopyranose were higher in DLT than YKT. Additionally, abundant hydrolyzable tannins are the characteristic phenolic constituents of DLT.

Pathway analysis revealed that the differential metabolites between DLT and YKT were primarily enriched in flavonoid biosynthesis. Genome data indicated that during the evolution of tea plant, genes associated with flavonoid metabolic biosynthesis were expanded, which including *FNSII*, *C4H*, *CHS*, *ANS*, *ANR*, and *F4'ST* (Xia et al., 2017; Zhang et al., 2015). Our metabolic data further revealed that when compared to DLT, YKT exhibited higher levels of flavonoid metabolites, such as kaempferol glycosides, quercetin glycosides, myricetin glycosides, and apigenin glycosides. Fang et al. reported that flavonol glycoside accumulation is primarily influenced by the genetic

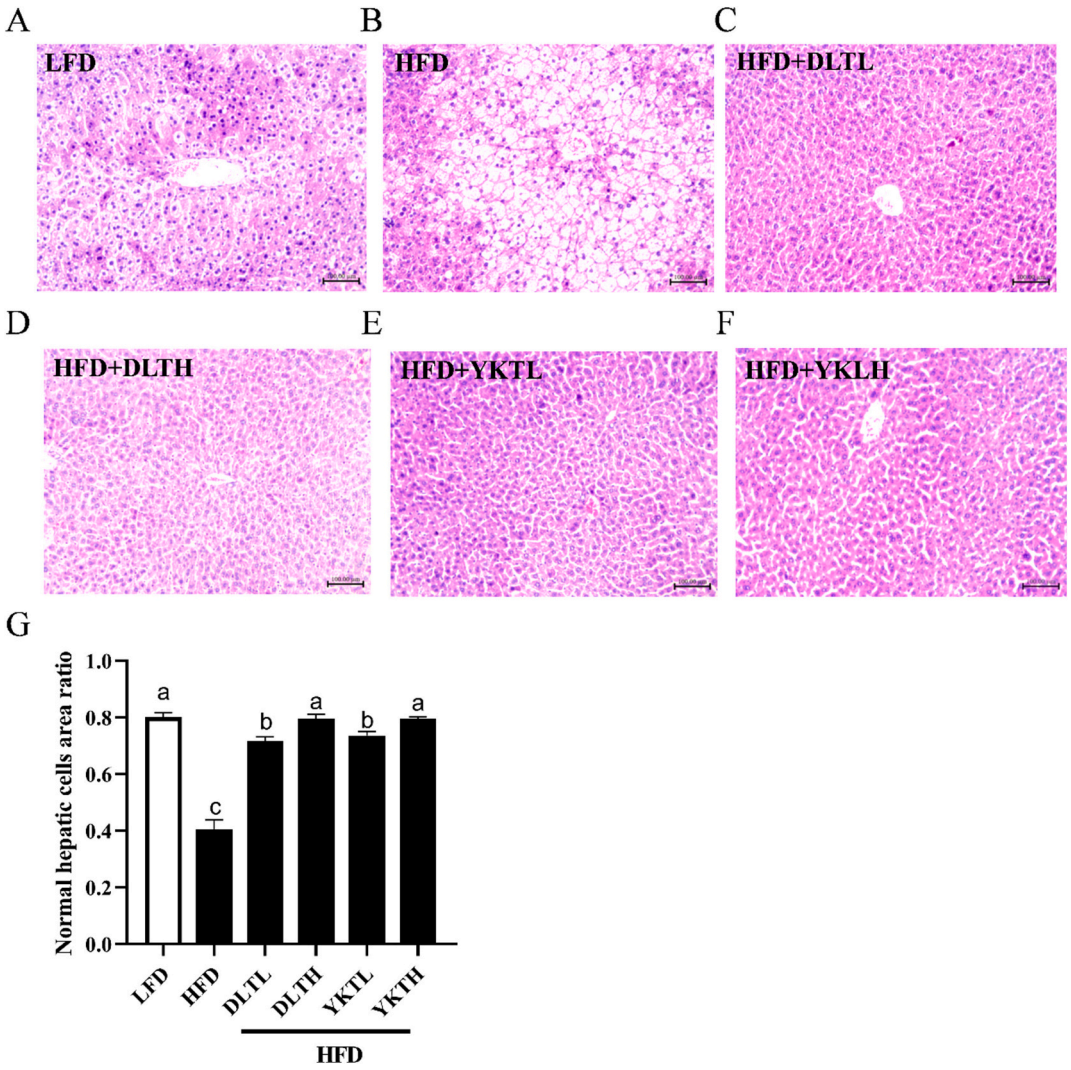

Fig. 8. DLT and YKT prevent fatty liver formation in HFD-fed mice.
Representive liver tissure images of LFD group (A), HFD group (B), HFD plus DLTL group (C), HFD plus DLTH group (D), HFD plus YKTL group (E), HFD plus YKTH group (F), and quantification of noral hepatic cess area across group (G), are showing. Different lowercase letters in each column indicate significant differences among groups ($p < 0.05$). All data are presented as mean ± SEM ($n = 3$).

background of tea trees (Fang et al., 2021). The reason that cultivated tea plants made YKT contain more flavonoids metabolites than wild tea plants made DLT may be the result of natural selection and domestication of tea plant.

Recently, natural products have gained attention for their potential role in alleviating obesity. Tea also exhibited anti-obesity effects. Tea consumption is associated with modulation of fat reduction and weight loss in humans and animals. To the best of our knowledge, this is the first preliminary study to evaluate the effectiveness of DLT supplements in reducing body weight and fat mass compared to YKT. Treatment of HFD feeding mice with DLT and YKT, a dose-dependent reduction in adiposity was observed, and YKT was found to be more effective on hypoadiposity than DLT at the same dosage. Tea catechins, especially epigallocatechin gallate have been shown to reduce obesity in both rats and humans (Gu et al., 2022; Patial et al., 2023). A meta-analysis also showed that flavonoids supplement improved overweight in controlled trials (Yao et al., 2022). Our chemical analysis data suggested that the abundance of catechins and flavonoids is higher in YKT than in DLT. *C/ebp α*, *Srebp-1c* and *Fas* are all key regulators for lipogenesis. Previously, Lim et al. reported that anti-obesity effects of dark tea extracts by down-regulation of C/EBPα (Lim et al., 2022). And Pu-erh tea suppresses diet-induced body fat accumulation in C57BL/6 J mice by down-regulating SREBP-1c and related molecules (Shimamura et al., 2013). In addition, Oolong tea extract alleviates weight gain in high-fat diet-induced obese rats by downregulated SREBP1 and FASN (Tung et al., 2022). Our gene expression study also showed that YKT exibites better inhibitory effects that DLT in attenuating *C/ebp α*, *Srebp-1c* and *Fas* expression in liver of HFD-mice. This may be a reason why YKT has better hypo-adiposity than DLT.

Metabolic associated fatty liver disease (MAFLD) is rapidly becoming the most common cause of chronic liver disease due to an increase in the prevalence of obesity. The development of MAFLD leads to an increase in morbidity and mortality. Therefore, findings of dietary approaches to prevent MAFLD are critical importance. Our previous paper reported that dietary supplement of large yellow tea attenuates hepatic steatosis in db/db mice (Teng et al., 2018). Green tea consumption is also promising to prevent MAFLD in animal models and human population (Zhou et al., 2019). Similar to these results, current study indicated that both YKT and DLT treatment significantly prevented lipid dispersition in liver tissues. Furthermore, HFD induced obese mouse is a type 2 diabetic animal, and consequently develops diabetic Nephropathy, A published paper reported that green tea prevented diabetic nephropathy of male db/db mice. In addition, white tea was found to improve the structural changes of the kidneys, such as glomerular hypertrophy, glomerular

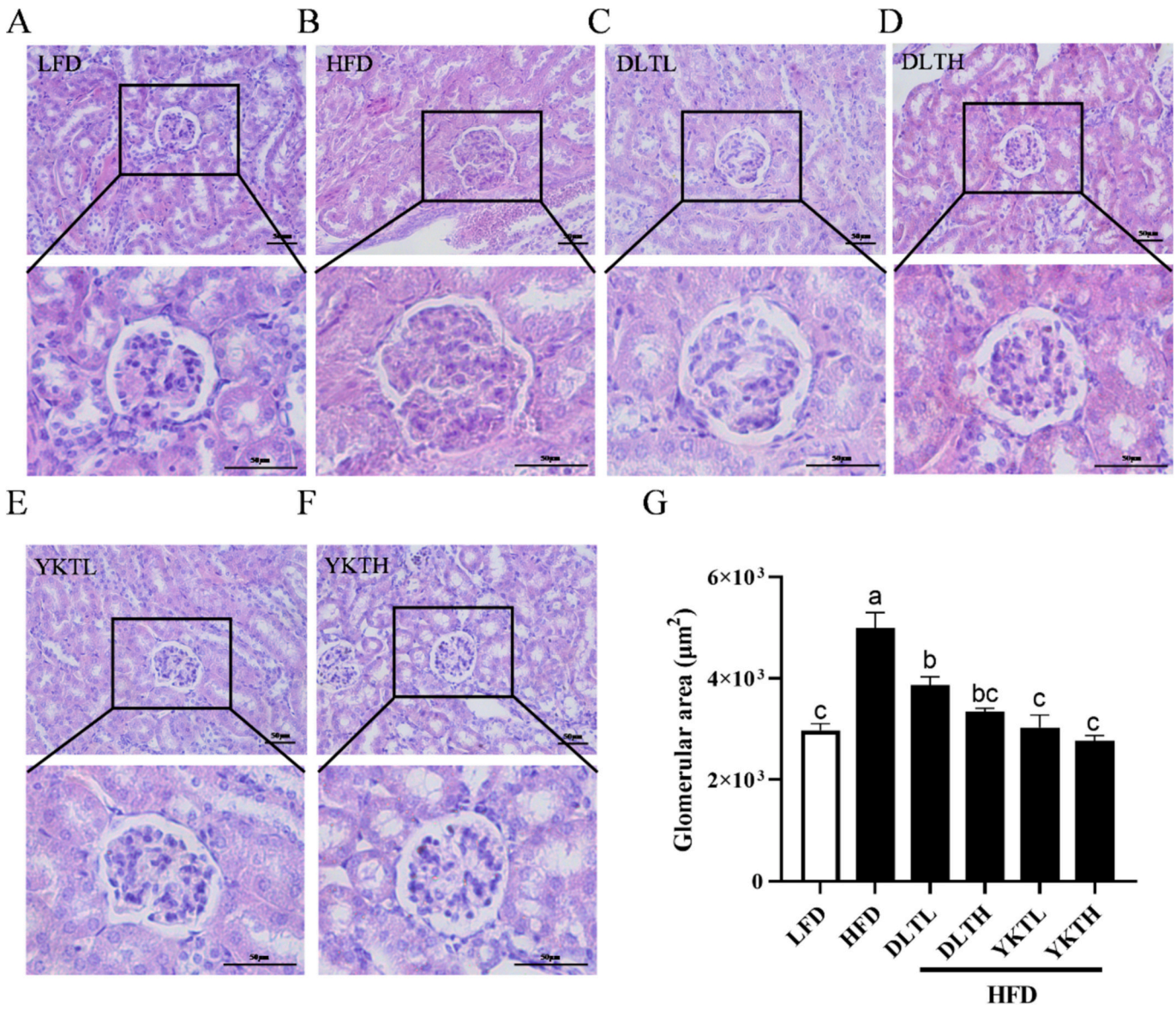

Fig. 9. Distinct protective effects for renal injury between DLT and YKT in HFD-fed mice.
(a)Representative HE staining of glomeruli structure of LFD group (A), HFD group (B), HFD plus DLTL group (C), HFD plus DLTH group (D), HFD plus YKTL group (E), HFD plus YKTH group (F). and quantification of noral hepatic cess area across group (G), and quantification of glomerular area in HE–stained kidney sections, with 30 glomerular sections in each group (G). Different lowercase letters in each column indicate significant differences among groups ($p < 0.05$). Values are presented as mean ± SEM ($n = 4–5$).

basement membrane thickening and kidney fibrosis in HFD combined with streptozotocin (STZ)-induced type 2 diabetic mice (Xia et al., 2021). Here, we comparatively investigated protective effects of YLT and DLT on mitigating abnormal renal hypertrophy and enhancing glomerular structural integrity. We found that both YKT and DLT can alleviate the renal lesions. Interestingly, YKT performed better preventive effects than that of DLT.

In summary, this study provided the first set of metabolite signatures of DLT compared to YKT. Animal study indicated that DLT is less effective on hypoadiposity and renal lesions in HFD induced obese mice than that of YKT. Our data revealed that DLT has more abundant amount of phenolic acid metabolites and hydrophilic amino acids than that of YKT, which may contribute to more profound resistance to abiotic stress of Dali species. Therefore, hybridization between Dali species with cultivated Assam tea plant would be a better strategy to improve nutrition value and resistance to abiotic stress of tea plants.

Funding

This research was funded by the National Key Research and Development Program of China (2021YFD1601102), Research Funds of Joint Research Center for Food Nutrition and Health of IHM (Grant numbers: 2023SJY02), and Earmarked Found for CARS (Grant numbers: CARS-19).

CRediT authorship contribution statement

Mengwan Li: Writing – original draft, Software, Methodology, Investigation, Formal analysis, Data curation. **Dan Liu:** Software, Methodology, Investigation, Formal analysis, Data curation. **Tingting Han:** Data curation, Formal analysis, Investigation. **Juan Li:** Software, Investigation, Data curation. **Linbo Chen:** Software, Resources, Formal analysis, Data curation. **Daxiang Li:** Writing – review & editing, Supervision, Funding acquisition, Conceptualization. **Zhongwen Xie:**

Writing – review & editing, Supervision, Project administration, Funding acquisition, Conceptualization.

Declaration of competing interest

The authors declare that they have no known competing financial interests or personal relationships that could have appeared to influence the work reported in this paper.

Appendix A. Supplementary data

Supplementary data to this article can be found online at https://doi.org/10.1016/j.fochx.2024.101989.

Data availability

Data will be made available on request.

References

Fang, Z. T., Yang, W. T., Li, C. Y., Li, D., Dong, J. J., Zhao, D., Xu, H. R., Ye, J. H., Zheng, X. Q., Liang, Y. R., & Lu, J. L. (2021). Accumulation pattern of catechins and flavonol glycosides in different varieties and cultivars of tea plant in China. *Journal of Food Composition and Analysis, 97*, Article 103772. https://doi.org/10.1016/j.jfca.2020.103772

Gao, D. F., Zhang, Y. J., Yang, C. R., Chen, K. K., & Jiang, H. J. (2008). Phenolic antioxidants from green tea produced from Camellia taliensis. *Journal of Agricultural and Food Chemistry, 56*(16), 7517–7521. https://doi.org/10.1021/jf800878m

Garay-Arroyo, A., Colmenero-Flores, J. M., Garciarrubio, A., & Covarrubias, A. A. (2000). Highly hydrophilic proteins in prokaryotes and eukaryotes are common during conditions of water deficit. *The Journal of Biological Chemistry, 275*(8), 5668–5674. https://doi.org/10.1074/jbc.275.8.5668

Gu, Q., Wang, X., Xie, L., Yao, X., Qian, L., Yu, Z., & Shen, X. (2022). Green tea catechin EGCG could prevent obesity-related precocious puberty through NKB/NK3R signaling pathway. *The Journal of Nutritional Biochemistry, 108*, Article 109085. https://doi.org/10.1016/j.jnutbio.2022.109085

Kim, S., Chen, J., Cheng, T., Gindulyte, A., He, J., He, S., … Bolton, E. E. (2023). PubChem 2023 update. *Nucleic Acids Research, 51*(D1), D1373–D1380. https://doi.org/10.1093/nar/gkac956

Li, D., Wang, R., Huang, J., Cai, Q., Yang, C. S., Wan, X., & Xie, Z. (2019). Effects and mechanisms of tea regulating blood pressure: Evidences and promises. *Nutrients, 11*(5), 1115. https://doi.org/10.3390/nu11051115

Li, M., Luo, X., Ho, C. T., Li, D., Guo, H., & Xie, Z. (2022). A new strategy for grading of Lu'an guapian green tea by combination of differentiated metabolites and hypoglycaemia effect. *Food research international (Ottawa, Ont.), 159*, Article 111639. https://doi.org/10.1016/j.foodres.2022.111639

Li, M., Shen, Y., Ling, T., Ho, C. T., Li, D., Guo, H., & Xie, Z. (2021). Analysis of differentiated chemical components between Zijuan purple tea and yunkang green tea by UHPLC-Orbitrap-MS/MS combined with chemometrics. *Foods, 10*(5), 1070. https://doi.org/10.3390/foods10051070

Liang, X., Wang, Y., Li, Y., An, W., He, X., Chen, Y., Shi, Z., He, J., & Wan, R. (2022). Widely-targeted metabolic profiling in Lyciumbarbarum fruits under salt-alkaline stress uncovers mechanism of salinity tolerance. *Molecules, 27*(5), 1564. https://doi.org/10.3390/molecules27051564

Lim, H., Lim, T., Lee, J., Lee, J. H., Kim, M., Park, J., Kim, J., Kim, M., Jang, S., & Choi, S. (2022). Anti-obesity effects of dark tea extracts by Down-regulation of C/EBPα and PPARγ. *In Vivo, 36*(4), 1753–1760. https://doi.org/10.21873/invivo.12888

Liu, Y., Yang, S. X., Ji, P. Z., & Gao, L. Z. (2012). Phylogeography of *Camellia taliensis* (Theaceae) inferred from chloroplast and nuclear DNA: Insights into evolutionary history and conservation. *BMC Evolutionary Biology, 12*, 92. https://doi.org/10.1186/1471-2148-12-92

Liu, Y., Zhao, G., Li, X., Shen, Q., Wu, Q., Zhuang, J., Zhang, X., Xia, E., Zhang, Z., Qian, Y., Gao, L., & Xia, T. (2020). Comparative analysis of phenolic compound metabolism among tea plants in the section Thea of the genus Camellia. *Food Research International, 135*, Article 109276. https://doi.org/10.1016/j.foodres.2020.109276

Meng, X. H., Li, N., Zhu, H. T., Wang, D., Yang, C. R., & Zhang, Y. J. (2019). Plant resources, chemical constituents, and bioactivities of tea plants from the genus Camellia section Thea. *Journal of Agricultural and Food Chemistry, 67*(19), 5318–5349. https://doi.org/10.1021/acs.jafc.8b05037

Meyer, R. S., Whitaker, B. D., Little, D. P., Wu, S. B., Kennelly, E. J., Long, C. L., & Litt, A. (2015). Parallel reductions in phenolic constituents resulting from the domestication of eggplant. *Phytochemistry, 115*, 194–206. https://doi.org/10.1016/j.phytochem.2015.02.006

Pang, Z., Zhou, G., Ewald, J., Chang, L., Hacariz, O., Basu, N., & Xia, J. (2022). Using MetaboAnalyst 5.0 for LC-HRMS spectra processing, multi-omics integration and covariate adjustment of global metabolomics data. *Nature Protocols, 17*(8), 1735–1761. https://doi.org/10.1038/s41596-022-00710-w

Patial, V., Katoch, S., Chhimwal, J., Dadhich, G., Sharma, V., Rana, A., Joshi, R., & Padwad, Y. (2023). Catechins prevent obesity-induced kidney damage by modulating PPARγ/CD36 pathway and gut-kidney axis in rats. *Life Sciences, 316*, Article 121437. https://doi.org/10.1016/j.lfs.2023.121437

Pollastri, S., & Tattini, M. (2011). Flavonols: Old compounds for old roles. *Annals of Botany, 108*(7), 1225–1233. https://doi.org/10.1093/aob/mcr234

Shimamura, Y., Yoda, M., Sakakibara, H., Matsunaga, K., & Masuda, S. (2013). Pu-erh tea suppresses diet-induced body fat accumulation in C57BL/6J mice by down-regulating SREBP-1c and related molecules. *Bioscience Biotechnology and Biochemistry., 77*(7), 1455–1460. https://doi.org/10.1271/bbb.130097

Swaminathan, S., Das, A., Assefa, T., Knight, J. M., Da Silva, A. F., Carvalho, J. P. S., … Bhattacharyya, M. K. (2019). Genome wide association study identifies novel single nucleotide polymorphic loci and candidate genes involved in soybean sudden death syndrome resistance. *PLoS One, 14*(2), Article e0212071. https://doi.org/10.1371/journal.pone.0212071

Teng, Y., Li, D., Guruvaiah, P., Xu, N., & Xie, Z. (2018). Dietary supplement of large yellow tea ameliorates metabolic syndrome and attenuates hepatic steatosis in db/db mice. *Nutrients, 10*(1), 75. https://doi.org/10.3390/nu10010075

Tien, M. (1992). A REVISION OF CAMELLIA SECT. *THEA. Acta Botanica Yunnanica, 14*, 115–132.

Tung, Y. C., Liang, Z. R., Yang, M. J., Ho, C. T., & Pan, M. H. (2022). *Oolong tea extract alleviates weight gain in high-fat diet-induced obese rats by regulating lipid metabolism and modulating gut microbiota Food & Function, 13*(5), 2846–2856. https://doi.org/10.1039/d1fo03356e

Wang, L., Pan, D., Liang, M., Abubakar, Y. S., Li, J., Lin, J., … Chen, W. (2017). Regulation of anthocyanin biosynthesis in purple leaves of Zijuan tea (*Camellia* sinensis var. *kitamura*). *International Journal of Molecular Sciences, 18*(4), 833. https://doi.org/10.3390/ijms18040833

Wei, K., Wang, L., Zhou, J., He, W., Zeng, J. M., Jiang, Y. W., & Cheng, H. (2012). Comparison of catechins and purine alkaloids in albino and normal green tea cultivars (*Camellia* sinensis L.) by HPLC. *Food Chemistry, 130*, 720–724. https://doi.org/10.1016/j.foodchem.2011.07.092

Wishart, D. S., Guo, A., Oler, E., Wang, F., Anjum, A., Peters, H., … Gautam, V. (2022). HMDB 5.0: The human metabolome database for 2022. *Nucleic Acids Research, 50*(D1), D622–D631. https://doi.org/10.1093/nar/gkab10621

Wu, G., Sun, X., Cheng, H., Xu, S., Li, D., & Xie, Z. (2022). Large yellow tea extract ameliorates metabolic syndrome by suppressing lipogenesis through SIRT6/SREBP1 pathway and modulating microbiota in leptin receptor knockout rats. *Foods, 11*(11), 1638. https://doi.org/10.3390/foods11111638

Xia, E. H., Zhang, H. B., Sheng, J., Li, K., Zhang, Q. J., Kim, C., … Gao, L. Z. (2017). The tea tree genome provides insights into tea flavor and independent evolution of caffeine biosynthesis. *Molecular Plant, 10*(6), 866–877. https://doi.org/10.1016/j.molp.2017.04.002

Xia, X., Wang, X., Wang, H., Lin, Z., Shao, K., Xu, J., & Zhao, Y. (2021). Ameliorative effect of white tea from 50-year-old tree of *Camellia sinensis* L. (Theaceae) on kidney damage in diabetic mice via SIRT1/AMPK pathway. *Journal of Ethnopharmacology, 272*, Article 113919. https://doi.org/10.1016/j.jep.2021.113919

Xie, Z., Su, W., Liu, S., Zhao, G., Esser, K., Schroder, E. A., Lefta, M., Stauss, H. M., Guo, Z., & Gong, M. C. (2015). Smooth-muscle BMAL1 participates in blood pressure circadian rhythm regulation. *The Journal of Clinical Investigation, 125*, 324–336. https://doi.org/10.1172/JCI76881

Yan, K., Cui, M., Zhao, S., Chen, X., & Tang, X. (2016). Salinity stress is beneficial to the accumulation of Chlorogenic acids in honeysuckle (Lonicera japonica Thunb.). *Frontiers in Plant Science, 7*, 1563. https://doi.org/10.3389/fpls.2016.01563

Yao, J., Zhang, Y., Zhao, J., Wang, X. Z., Lin, Y. P., Sun, L., … Fan, G. J. (2022). Efficacy of flavonoids-containing supplements on insulin resistance and associated metabolic risk factors in overweight and obese subjects: A systematic review and meta-analysis of 25 randomized controlled trials. *Frontiers in Endocrinology, 13*, Article 917692. https://doi.org/10.3389/fendo.2022.917692

Yue, Y., Chu, G. X., Liu, X. S., Tang, X., Wang, W., Liu, G. J., … Bao, G. H. (2014). TMDB: A literature-curated database for small molecular compounds found from tea. *BMC Plant Biology, 14*, 243. https://doi.org/10.1186/s12870-014-0243-1

Zeng, C., Lin, H., Liu, Z., & Liu, Z. (2019). Analysis of young shoots of 'Anji Baicha' (Camellia sinensis) at three developmental stages using nontargeted LC-MS-based metabolomics. *Journal of Food Science, 84*(7), 1746–1757. https://doi.org/10.1111/1750-3841.14657

Zhang, H. B., Xia, E. H., Huang, H., Jiang, J. J., Liu, B. Y., & Gao, L. Z. (2015). De novo transcriptome assembly of the wild relative of tea tree (*Camellia taliensis*) and comparative analysis with tea transcriptome identified putative genes associated with tea quality and stress response. *BMC Genomics, 16*(1), 298. https://doi.org/10.1186/s12864-015-1494-4

Zhang, W., Alseekh, S., Zhu, X., Zhang, Q., Fernie, A. R., Kuang, H., & Wen, W. (2020). Dissection of the domestication-shaped genetic architecture of lettuce primary metabolism. *The Plant journal : for cell and molecular biology, 104*(3), 613–630. https://doi.org/10.1111/tpj.14950

Zhang, Y., Gu, M., Wang, R., Li, M., Li, D., & Xie, Z. (2020). Dietary supplement of Yunkang 10 green tea and treadmill exercise ameliorate high fat diet induced metabolic syndrome of C57BL/6J mice. *Nutrition & Metabolism, 17*, 14. https://doi.org/10.1186/s12986-020-0433-9

Zhao, D. W., Yang, J. B., Yang, S. X., Kato, K., & Luo, J. P. (2014). Genetic diversity and domestication origin of tea plant Camellia taliensis (Theaceae) as revealed by

microsatellite markers. *BMC Plant Biology, 14*, 14. https://doi.org/10.1186/1471-2229-14-14

Zhou, J., Ho, C. T., Long, P., Meng, Q., Zhang, L., & Wan, X. (2019). Preventive efficiency of green tea and its components on nonalcoholic fatty liver disease. *Journal of Agricultural and Food Chemistry, 67*(19), 5306–5317. https://doi.org/10.1021/acs.jafc.8b05032

Zhu, L. F., Xu, M., Zhu, H. T., Wang, D., Yang, S. X., Yang, C. R., & Zhang, Y. J. (2012). New flavan-3-ol dimer from green tea produced from Camellia taliensis in the Ai-Lao mountains of Southwest China. *Journal of Agricultural and Food Chemistry, 60*(49), 12170–12176. https://doi.org/10.1021/jf302726t